ELSEVIER

Journal of Power Sources 108 (2002) 250–255

JOURNAL OF POWER SOURCES

www.elsevier.com/locate/jpowsour

Short communication

Synthesis and characterization of multidoped lithium manganese oxide spinel, $Li_{1.02}Co_{0.1}Ni_{0.1}Mn_{1.8}O_4$, for rechargeable lithium batteries

B.J. Hwang*, R. Santhanam, S.G. Hu

Department of Chemical Engineering, Microelectrochemistry Laboratory, National Taiwan University of Science and Technology, 43 Keelung Road, Sec. 4, 106 Taipei, Taiwan, ROC

Received 15 August 2001; accepted 4 January 2002

Abstract

A multidoped spinel, $LiCo_xNi_yMn_{2-x-y}O_4$ ($x = y = 0.1$), that is of interest as a cathode material for rechargeable lithium batteries has been synthesized by the sol–gel method and characterized by X-ray diffraction (XRD) and electrochemical methods. Electrochemical experiments show that compared with Ni-doped spinel, Co-doped spinel delivers higher initial capacity, but its rate capability is poor. It is interesting to note that the initial capacity is enhanced, significantly when Co is doped into the Ni-doped spinel $LiMn_2O_4$, while the rate capability is retained. In other words, the multidoped spinel, $LiCo_xNi_yMn_{2-x-y}O_4$ shows the best features of the single-doped spinels, $LiCo_xMn_{2-x}O_4$ and $LiNi_yMn_{2-y}O_4$. Voltage versus capacity studies indicate that the phase transitions are reduced significantly for the multidoped spinel, $LiCo_xNi_yMn_{2-x-y}O_4$, during charging and discharging. X-ray diffraction data reveal that the diffraction peak intensity ratio of the typical peaks for the cubic phase (3 1 1) and (4 0 0), does not change after charging for the multidoped spinel, $LiCo_xNi_yMn_{2-x-y}O_4$. This suggests that cation disordering is completely prevented in this multidoped spinel material.

Keywords: Multidoped spinel; Rechargeable lithium batteries; Electric vehicle applications

1. Introduction

Spinel lithium manganese oxide, $Li_xMn_2O_4$, and its derivatives are considered as promising cathode materials for rechargeable lithium batteries because of their advantages such as low cost, non-toxicity, abundance and relatively high specific energy [1–5]. Spinel $Li_xMn_2O_4$ mainly exhibits two voltage plateaus, namely 4 V for $0 < x \leq 1$ and 3 V for $1 < x \leq 2$. The cubic structure of the spinel $LiMn_2O_4$ is maintained when it is cycled in the 4 V range. On the other hand, a severe capacity fading is observed in the 3 V range due to structural phase transformation from cubic to tetragonal, due to Jahn–Teller distortion of Mn^{3+} ions. Even though the cycling performance of the spinel $LiMn_2O_4$ electrode is far better in the 4 V range than the 3 V range, it shows considerable capacity fading in the 4 V range also, on long-term cycling. This capacity fading is mainly attributed to dissolution of spinel into the electrolyte and decomposition of the electrolyte [6–8]. Many authors have also proposed, that the inferior cycleability of the $LiMn_2O_4$ spinel is due to cation mixing between Li and Mn ions in the spinel lattice [9,10], breakdown of the spinel lattice [11,12], and oxygen loss from the spinel lattice [13–16]. Extensive studies have been carried out on various approaches to overcome these problems and hence to improve the cycleability of the spinel $LiMn_2O_4$. Among these, one effective approach is to substitute a small amount of dopant ions instead of Mn ions [17–21]. It is believed that the dopant ions are occupied in the 16d sites of Mn-ions in the spinel lattice and stabilize the spinel structure.

Three major issues should be solved in order to use $LiMn_2O_4$ spinel material in commercial lithium batteries. They are: (1) capacity fading during prolonged cycling; (2) decrease in the initial capacity; (3) low rate capability. Spinel $LiMn_2O_4$ doped with single metal ions either offers a high capacity similar to the practical capacity obtained from undoped spinel cathode [22], but with limited cycleablility upon cycling, or offers relatively stable cycle-life but low initial capacity [20,23]. In this work, our intention is to synthesize a multidoped spinel material that exhibits the beneficial features of both single-doped spinels. For this purpose, we synthesize a multidoped spinel $LiCo_xNi_yMn_{2-x-y}O_4$ and examine its battery performance. Spinels doped with single metal ions, i.e. $LiCo_xMn_{2-x}O_4$, and $LiNi_yMn_{2-y}O_4$, have also been synthesized and their

* Corresponding author. Tel.: +886-2-27376624; fax: +886-2-27376644.
E-mail address: bjh@ch.ntust.edu.tw (B.J. Hwang).

0378-7753/02/$ – see front matter
PII: S0378-7753(02)00023-X

characteristics are compared with multidoped spinel. Since rate capability is very important for electric vehicle (EV) applications, the battery characteristics of all these spinels are studied at low as well as high C-rates.

2. Experimental

All the samples, $LiMn_2O_4$, $LiCo_xMn_{2-x}O_4$, and $LiNi_yMn_{2-y}O_4$, and $LiCo_xNi_yMn_{2-x-y}O_4$ were synthesized by the citric acid sol–gel method [24,25]. Stoichiometric amounts of: (1) $Li(CH_3COO)\cdot 4H_2O$ and $Mn(CH_3COO)_2\cdot 4H_2O$; (2) $Li(CH_3COO)\cdot 4H_2O$, $Mn(CH_3COO)_2\cdot 4H_2O$, $Ni(CH_3COO)_2\cdot 4H_2O$ and $Co(NO_3)_2\cdot 4H_2O$, were dissolved in distilled water. Citric acid was used as a chelating agent. The temperature was maintained at 35 °C. The solution pH was adjusted to 6.0 with ammonium hydroxide. The entire process was carried out under continuous stirring. The prepared solution was heated in a beaker on a hot plate in the temperature range 80–90 °C for 4 h until a transparent sol was obtained. The resulting gel precursor was decomposed at 400 °C for 4 h in oxygen to remove the organic contents. The decomposed powders were ground, pressed into pellets and calcined at 800 °C in oxygen for 10 h. The heating rate of the powder was 2 °C/min.

The Li, Co, Ni and Mn contents in the resulting materials were analyzed, using an inductively coupled plasma/atomic emission spectrometer (ICP/AES, Kontron S-35). Phase purity was verified by powder X-ray diffraction (XRD; Rigaku $D/\max - b$) using Cu Kα radiation. Electrochemical characterization was carried out with coin-type cells. The cathode was prepared by mixing 85/3.5/1.5/10 (w/w) ratio of active material, carbon black, KS6 graphite and polyvinylidene fluoride binder, respectively, in *N*-methyl pyrrolidinone. The resulting paste was applied to a aluminium current-collector. The entire assembly was dried under vacuum overnight and then heated in an oven at 120 °C for 2 h. Lithium metal (Aldrich) was used as an anode and a polypropylene separator was inserted between the anode and the cathode. The electrolyte was 1.0 M $LiPF_6$ dissolved in a 1/1 mixture of ethylene carbonate (EC)/diethyl carbonate (DEC). The cells were assembled in an argon-filled dry box in which the content of both moisture and oxygen was <1 ppm. Charge and discharge cycles were carried out at low and high charging and discharging rates (C-rates), namely, 0.3 and 1.0 C, over a potential range between 3.3 and 4.3 V.

3. Results and discussion

From ICP-AES analysis, the composition of the synthesized samples was found to be $Li_{1.02}Mn_2O_4$, $Li_{1.02}Co_{0.1}Mn_{1.9}O_4$, $Li_{1.02}Ni_{0.1}Mn_{1.9}O_4$ and $Li_{1.02}Co_{0.1}Ni_{0.1}Mn_{1.8}O_4$. The structures of all these samples were characterized using XRD. The XRD patterns of as-prepared samples, namely, undoped spinel, Co-doped spinel, Ni-doped spinel and (Co, Ni)-doped spinel are shown in Fig. 1a–d, respectively. All the samples were synthesized under the same processing conditions as described in the experimental section by manipulating stoichiometric compositions of the corresponding starting materials. All the as-prepared samples have a well-defined spinel phase structure, as shown in Fig. 1.

The charge–discharge properties of all the as-prepared samples were examined by fabricating an electrode and assembling it in a coin cell, as described in Section 2, over

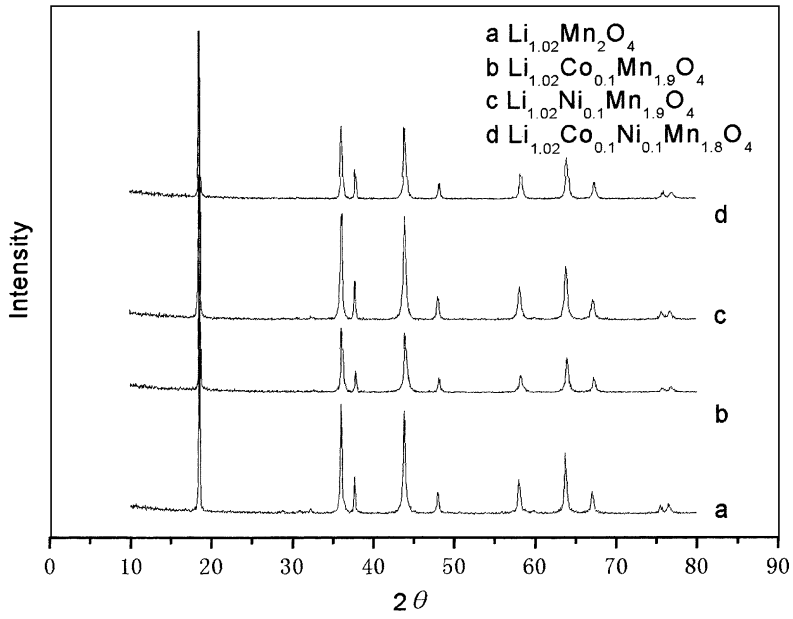

Fig. 1. XRD patterns of: (a) $Li_{1.02}Mn_2O_4$; (b) $Li_{1.02}Co_{0.1}Mn_{1.9}O_4$; (c) $Li_{1.02}Ni_{0.1}Mn_{1.9}O_4$ and (d) $Li_{1.02}Co_{0.1}Ni_{0.1}Mn_{1.8}O_4$ powders.

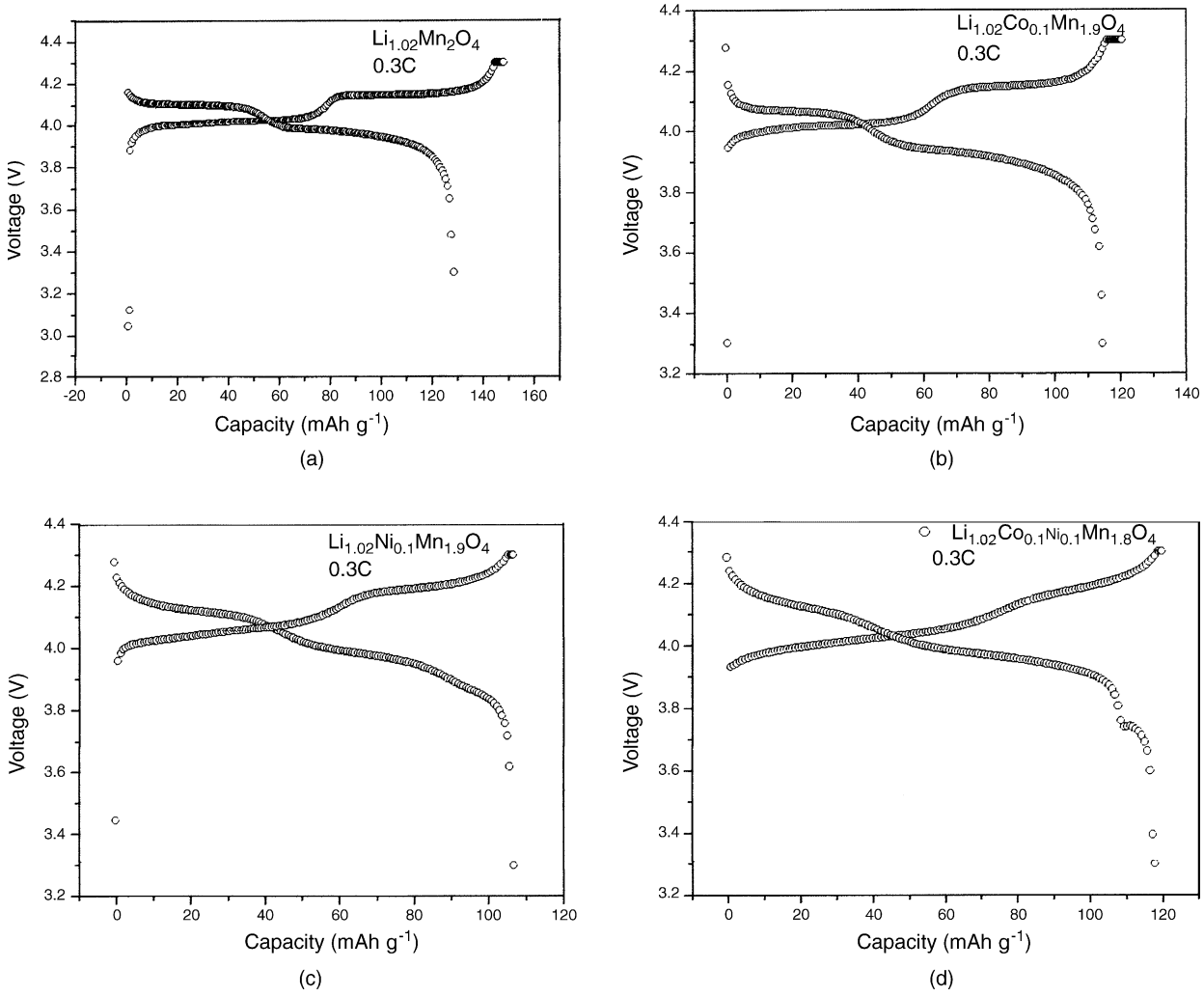

Fig. 2. Voltage vs. capacity profiles obtained during charging and discharging of: (a) $Li_{1.02}Mn_2O_4$; (b) $Li_{1.02}Co_{0.1}Mn_{1.9}O_4$; (c) $Li_{1.02}Ni_{0.1}Mn_{1.9}O_4$ and (d) $Li_{1.02}Co_{0.1}Ni_{0.1}Mn_{1.8}O_4$ cathodes.

a potential range between 3.3 and 4.3 V at 0.3 C. The charge–discharge curves for the first cycles of the as-prepared samples, undoped spinel, Co-doped spinel, Ni-doped spinel and (Co, Ni)-doped spinel, are shown in Fig. 2a–d, respectively. Undoped spinel has two well-defined plateaus (Fig. 2a). At the beginning of the charging, the curve is a steep slope. Then, the first plateau appears until about 4.1 V; a step is seen from 4.1 to 4.15 V. The second plateau appears after this step. At the end of charge, a steep slope occurs again. All these observations are almost reversible during discharge, as can be seen in the discharge curve of Fig. 2a. The charge–discharge behavior of $Li_{1.02}Mn_2O_4$ presented here is in good agreement with the three-phase model proposed recently by Yang et al. [26] from in situ synchrotron XRD studies. The steep slope region during the beginning of charge is assigned to phase I. The first plateau is attributed to a co-existence region between phase I + phase II. The step between the two plateaus is assigned to a single phase II. The second plateau is assigned to co-existence region between phase II + phase III. When comparing the shapes of all the as-prepared samples, namely, undoped, Co-doped, Ni-doped and (Co, Ni)-doped spinels $Li_{1.02}Mn_2O_4$, the (Co, Ni)-doped sample seems to reduce the phase transitions or maintain a relatively single phase with a very small voltage change around 4.1 V.

The discharge capacities and percentage of capacity fading rate of the undoped, Co-doped, Ni-doped and (Co, Ni)-doped spinels at as a function of cycle number and C-rate are shown in Table 1. It should be noted, that there is a great difference in the discharge capacity versus cycle number between these samples (Fig. 3). The discharge capacity of the undoped spinel sample abruptly declines to 78 mAh g^{-1} at the 40th cycle at 0.3 C, but for all the other three doped samples the capacity retention is good until 40 cycles at the same C-rate. As mentioned in the experimental section, from 40 to 80 cycles a high C-rate, viz. 1.0 C was used. For the undoped sample, the discharge capacity decreases only slowly and reaches 56 mAh g^{-1} after 80 cycles. When comparing the high C-rate performance of Co-doped and Ni-doped samples, the capacity retention of the Ni-doped

Table 1
Discharge capacities and percentage of capacity fading rate of bare, Co-doped, Ni-doped and (Co, Ni)-doped $LiMn_2O_4$ spinel

Samples	Discharge capacity (mAh g^{-1})			Capacity fading rate (%)	
	Initial	40th cycle	80th cycle	40th cycle	80th cycle
$Li_{1.02}Mn_2O_4$	139	78	56	43.8	59.7
$Li_{1.02}Co_{0.1}Mn_{1.9}O_4$	114	100	18	12.3	84.2
$Li_{1.02}Ni_{0.1}Mn_{1.9}O_4$	107	101	91	5.6	14.9
$Li_{1.02}Co_{0.1}Ni_{0.1}Mn_{1.8}O_4$	118	109	88	7.6	25.4

1–40 cycles at 0.3 C and 41–80 cycles at 1.0 C.

sample is significantly better. By contrast, the initial capacity of the Co-doped sample is higher than that of the Ni-doped sample. High initial capacity and capacity retention are the main requirements for the cathode materials to achieve good battery performance and (Co, Ni)-doped spinel satisfies these requirements. Although Ni-doped spinel shows high capacity retention, the initial capacity is lower than that of the (Co, Ni)-doped spinel. On the other hand, undoped and Co-doped spinels give higher initial capacity than the Ni-doped sample but the capacity fading is more. The higher initial capacity with excellent capacity retention of the (CO, Ni)-doped sample at low and high C-rates may be due to a synergetic action of the Co and Ni ions. The structure of $LiMn_2O_4$ spinel is stabilized as the Co ions deliver high initial capacity and the Ni ions maintain good capacity retention.

The XRD patterns of all the as-prepared samples show peaks that are typical for a cubic spinel structure (Fig. 1). The structures of all samples were evaluated after charge–discharge cycling to ascertain, why the doped samples show less capacity fading than the bare sample. For the XRD analysis, the samples were prepared by cycling the Li/undoped or doped spinel cell over a number of cycles. The cells were allowed to equilibrate for 4 h in the fully discharged state, and then disassembled. The spinel electrodes were removed from the cell and dried for 12 h in a dry box. The XRD patterns of the bare, Co-doped, and (Co, Ni)-doped spinels after cycling over a potential range between 3.3 and 4.3 V, are shown in Fig. 4a–d, respectively. There are no differences in the XRD peak characteristics of the cycled electrodes and the as-prepared samples, i.e. Co-doped, Ni-doped and (Co, Ni)-doped spinels. This observation indicates that the structure of the electrodes retains the original cubic phase, even after cycling for a number of cycles at low and high C-rates. By contrast, XRD pattern for the cycled $Li_{1.02}Mn_2O_4$ electrode change significantly. Peak broadening and peak splitting, which are the main characteristics of phase transitions of the sample, occur after cycling, as can be seen in Fig. 4a. Some impurity phases are also observed in this pattern.

Although there are no impurity phases, peak broadening and splitting in the XRD pattern after charging for the Co-doped, Ni-doped and (Co, Ni)-doped samples (Fig. 4), the intensity ratio of (3 1 1)/(4 0 0) diffraction peaks, which are

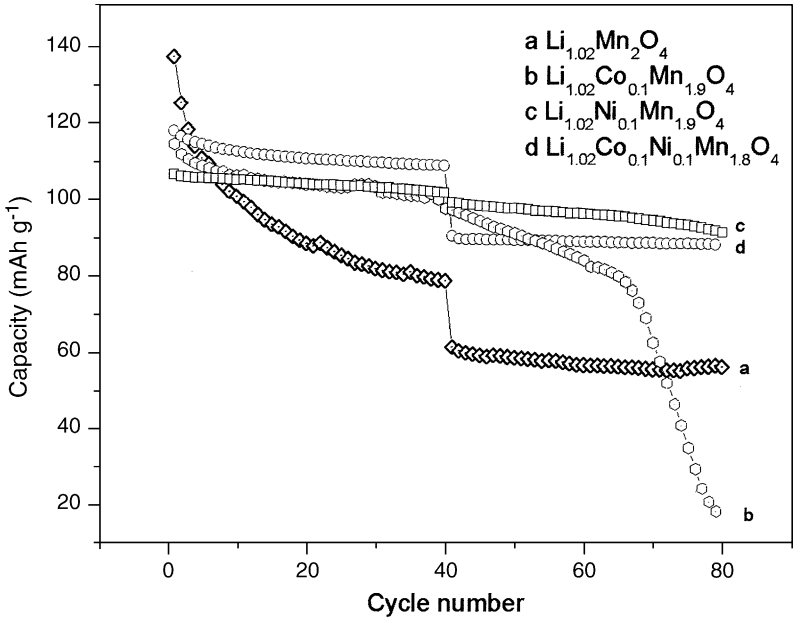

Fig. 3. Discharge capacity vs. cycle number for: (a) $Li_{1.02}Mn_2O_4$; (b) $Li_{1.02}Co_{0.1}Mn_{1.9}O_4$; (c) $Li_{1.02}Ni_{0.1}Mn_{1.9}O_4$ and (d) $Li_{1.02}Co_{0.1}Ni_{0.1}Mn_{1.8}O_4$ cathodes. One to forty cycles, 0.3 C and 41–80 cycles, 1.0 C.

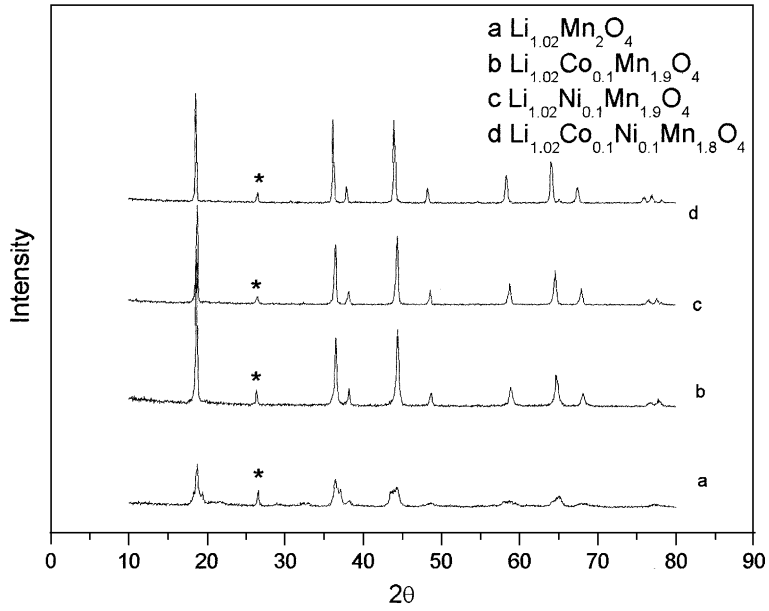

Fig. 4. XRD patterns of: (a) $Li_{1.02}Mn_2O_4$; (b) $Li_{1.02}Co_{0.1}Mn_{1.9}O_4$; (c) $Li_{1.02}Ni_{0.1}Mn_{1.9}O_4$ and (d) $Li_{1.02}Co_{0.1}Ni_{0.1}Mn_{1.8}O_4$ cathodes after 80 cycles. One to forty cycles at 0.3 C and 41–80 cycles at 1.0 C.

Table 2
Intensity ratio of (3 1 1)/(4 0 0) peaks of bare, Co-doped, Ni-doped and (Co, Ni)-doped $LiMn_2O_4$ spinel before and after charging

$Li_{1.02}Mn_2O_4$		$Li_{1.02}Co_{0.1}Mn_{1.9}O_4$		$Li_{1.02}Ni_{0.1}M_{1.9}O_4$		$Li_{1.02}Co_{0.1}Ni_{0.1}$ $Mn_{1.8}O_4$	
Before	After	Before	After	Before	After	Before	After
1.04	1.39	1.05	0.88	1.00	0.88	1.00	100

the typical peaks for the cubic phase, varies significantly for Co-doped and Ni-doped samples (Table 2). For the (Co, Ni)-doped sample, however, the intensity ratio of the (3 0 0)/(4 0 0) peaks is the same before and after charging. This indicates that the cation disordering in the (Co, Ni)-doped sample may be much less than that in the Co-doped and Ni-doped samples. Hence, the multidoped $Li_{1.02}Co_{0.1}Ni_{0.1}Mn_{1.8}O_4$ sample shows good capacity retention with high capacity at both low and high C-rates.

4. Conclusions

A multidoped spinel phase of $Li_{1.02}Co_{0.1}Ni_{0.1}Mn_{1.8}O_4$ has been synthesized by the sol–gel method. Studies suggest that this material can be used as a cathode material, for rechargeable lithium batteries, since it delivers a high initial capacity and shows excellent stability at both low and high C-rates. It gives 92% of the initial capacity after 40 cycles at a low C-rate (0.3 C) and 75% after 80 cycles at a high C-rate (1.0 C). Electrochemical and XRD measurements suggest, that the phase transitions are significantly reduced during charging and discharging and that cation disordering is completely prevented upon cycling. Further crystallographic studies on the multidoped Mn spinel material, would be worthwhile to determine why this multidoped material, $Li_{1.02}Co_{0.1}Ni_{0.1}Mn_{1.8}O_4$, shows excellent stability at low and high C-rates while delivering an initial capacity comparable with that of undoped Mn spinel.

Acknowledgements

The financial support from National Science Council (NSC 89-2214-E-011-044 and NSC 90-2811-E-011-005) and National Taiwan University of Science and Technology, Taiwan, Republic of China is gratefully acknowledged.

References

[1] S. Megahed, B. Scrosati, J. Power Sources 51 (1994) 79.
[2] J.M. Tarascon, E. Wang, F.K. Shokoohi, W.R. Mckinnon, S. Colson, J. Electrochem. Soc. 138 (1991) 2859.
[3] T. Ohzuku, M. Kitagawa, T. Hirai, J. Electrochem. Soc. 137 (1990) 769.
[4] J.M. Tarascon, D. Guyomard, J. Electrochem. Soc. 138 (1991) 2864.
[5] M.M. Thackeray, Prog. Solid State Chem. 25 (1997) 1.
[6] Y. Xia, Y. Zhou, M. Yoshio, J. Electrochem. Soc. 144 (1997) 2593.
[7] D.H. Jang, Y.J. Shin, S.M. Oh, J. Electrochem. Soc. 143 (1996) 2204.
[8] D.H. Jang, S.M. Oh, J. Electrochem. Soc. 144 (1997) 3342.

[9] J.M. Tarascon, W.R. Mckinnon, F. Coowar, T.N. Bowmer, G. Amatucci, D. Guyomard, J. Electrochem. Soc. 141 (1994) 1421.
[10] D. Guyomard, J.M. Tarascon, Solid State Ionics 69 (1994) 222.
[11] Y. Xia, M. Yoshio, J. Power Sources 57 (1995) 125.
[12] Y. Xia, M. Yoshio, J. Electrochem. Soc. 143 (1996) 825.
[13] Y. Gao, J.R. Dahn, Solid State Ionics 84 (1996) 33.
[14] Y. Gao, J.R. Dahn, J. Electrochem. Soc. 143 (1996) 100.
[15] H.H. Huang, C.A. Vincent, P.G. Bruce, J. Electrochem. Soc. 146 (1999) 481.
[16] Y. Xia, T. Sakai, T. Fujieda, X.Q. Yang, X. Sun, Z.F. Ma, J. McBreen, M. Yoshio, J. Electrochem. Soc. 148 (2001) A723.
[17] Y. Ein-Eli, J.T. Vaughty, M.M. Thackeray, S. Mukerjee, X.Q. Yang, J. Mcbreen, J. Electrochem. Soc. 146 (1999) 908.
[18] J.H. Lee, J.K. Hong, D.H. Jang, Y.K. Sun, S.M. Oh, J. Power Sources 89 (2000) 7.
[19] N. Hayashi, H. Ikuda, M. Wakihara, J. Electrochem. Soc. 146 (1999) 1351.
[20] Y. Ein-Eli, W.F. Howard, J. Electrochem. Soc. 144 (1997) L205.
[21] B.J. Hwang, R. Santhanam, D.G. Liu, Y.W. Tsai, J. Power Sources, 102 (2001) 326.
[22] Q. Zheng, A. Bonakdarpour, M. Zhang, Y. Gao, J.R. Dahn, J. Electrochem. Soc. 144 (1997) 205.
[23] Y. Ein-Eli, W.F. Howard, S.H. Lu, S. Mukerjee, J. McBreen, J.T. Vaughty, M.M. Thackeray, J. Electrochem. Soc. 145 (1998) 1238.
[24] J.H. Choy, D.H. Kim, C.W. Kwon, S.J. Hwang, Y.I. Kim, J. Power Sources 77 (1999) 1.
[25] B.J. Hwang, R. Santhanam, D.G. Liu, J. Power Sources 97/98 (2001) 443.
[26] X.Q. Yang, X. Sun, S.J. Lee, J. McBreen, S. Mukerjee, M.L. Daroux, X.K. Xing, Electrochem. Solid State Lett. 2 (1999) 157.